Biophysical Reports

REPORT

A trafficking motif alters GEVI activity implicating persistent protein interactions at the membrane

Sungmoo Lee,[1,2] Bok Eum Kang,[1] Yoon-Kyu Song,[2] and Bradley J. Baker[1,3,*]

[1]Brain Science Institute, Korea Institute of Science and Technology, Seoul, Republic of Korea; [2]Graduate School of Convergence Science and Technology, Seoul National University, Seoul, Republic of Korea; and [3]Division of Bio-Medical Science and Technology, KIST School, University of Science and Technology (UST), Seoul, Republic of Korea

ABSTRACT Efficient plasma-membrane expression is critical for genetically encoded voltage indicators (GEVIs). To improve the plasma-membrane expression, we introduced multiple combinations of plasma-membrane trafficking motifs at different positions to members of the Bongwoori family of GEVIs. An improvement from 20% to 27% in the ΔF/F/100 mV depolarization of the plasma membrane was observed when a Golgi transport motif was inserted near the N-terminus in conjunction with an endoplasmic reticulum release motif near the C-terminus of the protein. Unfortunately, this variant was also slower. The weighted tau on of the variant (25 ms) was more than double the original construct (11 ms). The weighted tau off was >20 ms compared with 10 ms for the original GEVI. The voltage range of the GEVI was also shifted to more negative potentials. Insertion of spacer amino acids between the fluorescent-protein domain and the endoplasmic reticulum release motif at the C-terminus rescued the speed of both the tau on and tau off while restoring the voltage range and maintaining the improved voltage-dependent optical signal. These results suggest that while trafficking motifs do improve plasma-membrane expression, they may also mediate persistent associations that affect the functioning of the protein.

WHY IT MATTERS The nervous system employs voltage changes to process and transmit information. Fluorescent proteins that alter their optical output in response to voltage changes enable the visualization of that process, improving our ability to study neuronal circuits. The addition of trafficking motifs that potentially improve the expression of the protein also altered its function. The speed of the optical response was slower, and the protein responded to a different voltage range. Inserting a flexible region into the protein at a precise position returned the speed and voltage range to the original version while improving the fluorescence change of the protein sensor, offering insights into how these fluorescent proteins work as well as providing a better fluorescent voltage sensor.

INTRODUCTION

The voltage-sensing domain (VSD) of a genetically encoded voltage indicator (GEVI) must reside in the plasma membrane since the electric field decreases dramatically with distance away from the cell membrane (1). Poor membrane expression of a GEVI decreases the number of photons responding to voltage transients thereby increasing the influence of the nonresponsive intracellular and intrinsic fluorescence and reducing the signal-to-noise ratio (2). Optimized membrane trafficking is therefore a paramount requirement for successful voltage imaging.

Cytoplasmic signal peptides from the inwardly rectifying potassium channel 2.1 (Kir2.1) have been identified to improve plasma-membrane expression of transgenes (Fig. 1 *A* and *B*) (3–9). A short seven amino acid motif (FCYENEV) from the C-terminus of Kir2.1 facilitates the endoplasmic reticulum (ER) to the Golgi apparatus transport (10–12). Motifs that enhance the transport of protein from the Golgi to the plasma membrane have also been identified in both the N-terminal (RSRFVKKDGHCNVQFINV; 18 aa) and C-terminal (KSRITSEGEYIPLDQIDINV; 20 aa) regions of the protein (13–16). Whereas removal of these amino acid motifs showed disruption of plasma-membrane expression of Kir2.1 in mammalian cells, transplanting the signals

Submitted December 12, 2021, and accepted for publication February 18, 2022.

*Correspondence: bradley.baker19@gmail.com

Sungmoo Lee Present address is Department of Neurobiology, Stanford University, Stanford, California, USA

Editor: Jörg Enderlein.

https://doi.org/10.1016/j.bpr.2022.100047

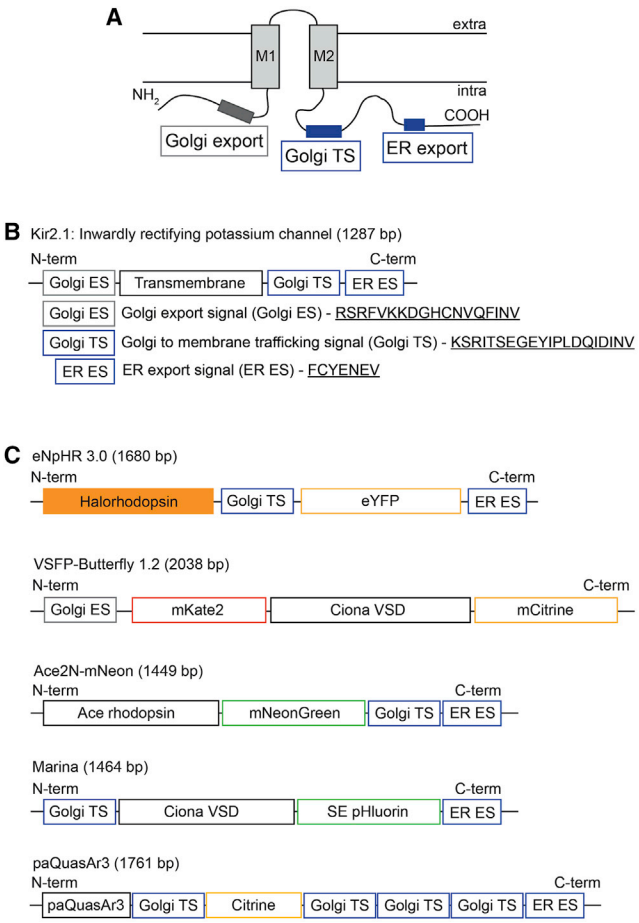

FIGURE 1 Composition of membrane-targeting sequences used in various optogenetic tools. (*A*) Schematic diagram and amino acid sequences of the three Kir2.1 membrane-trafficking motifs that are known to improve membrane targeting of the ion channel. (*B*) Protein sequences of the trafficking motifs. (*C*) Composition of Kir2.1-originated membrane-trafficking motifs introduced in representative optogenetic tools. The inhibitory optogenetic actuactor, eNpHR3.0, used the Golgi-to-membrane trafficking signal (Golgi TS) and the ER export signal (ER ES) before and after its reporter FP, respectively. For voltage-sensitive fluorescent protein butterfly 1.2, the Golgi export signal (Golgi ES) was located at the N-terminus. Ace2N-mNeon has Golgi TS and ER ES in tandem at the C-terminus to preserve the distance between the rhodopsin and the FP for electrochromic FRET. The Golgi TS and ER ES were placed at the N- and C- termini for Marina. Finally, paQuasAr3 used four Golgi TS flanking its fluorescent reporter (Citrine) and an ER ES at the C-terminus. SE pHluorin, super ecliptic pHluorin.

was shown to improve ER and Golgi exports of other membrane proteins (10,11,14,17).

The independent nature of these trafficking motifs has led to an empirical approach exploring different combinations to improve plasma-membrane expression (Fig. 1 *C*) since the combination that works for one protein does not necessarily transfer to another. For instance, a trafficking motif may affect protein folding depending on where it is introduced and how it affects the secondary and tertiary structures of the protein. Also, these motifs need to be accessible to the trafficking machineries of the cell, and this requires distinct optimal positions for different proteins.

Two membrane-trafficking motifs have been widely used by many optogenetic tools. Halorhodopsin induces a light-dependent chloride influx when expressed in neurons, enabling experimental control of neuronal inhibition (18), but suffered from poor membrane expression (3,4). Addition of the Golgi to the plasma membrane trafficking signal (Golgi TS) and the ER export signal (ER ES) from the C-terminus of Kir2.1 improved membrane expression (4). The voltage-sensitive fluorescent protein butterfly 1.2 has the Golgi export signal (Golgi ES) from the N-terminus of Kir2.1 upstream of its Förster resonance Energy transfer (FRET) acceptor, mKate2 (5). For an electrochromic FRET version microbial opsin GEVI, Ace2N-mNeon, both Golgi TS and ER ES were inserted after the fluorescent protein (FP), mNeonGreen, in tandem so as to not disturb the FRET between the opsin and the FP (7). In GEVIs with a classic VSD such as Arc-Light-mt (a membrane-trafficking optimized version of ArcLight) (19,20) and Marina (6), the Golgi TS was inserted upstream of the transmembrane segment, S1, of the VSD, while the ER ES was placed at the C-terminus. Finally, paQuasAr3, an opsin-only GEVI, used four Golgi TS motifs and one ER ES placed downstream of the voltage indicator (8). These examples suggest that different GEVI designs may require altered locations for trafficking motifs for optimum membrane expression. This is also true for the use of a 65-amino-acid-long, soma-targeting motif derived from the voltage-gated potassium channel 2.1 (Kv2.1) in various GEVIs (21–24).

Here, we tested different combinations and locations of the membrane-trafficking motifs from Kir2.1 in the Bongwoori family of GEVIs (25,26). The Golgi TS and the ER ES were introduced either separately or jointly in several regions of Bongwoori-R3 and -Pos6. Bongwoori-R3 with both Golgi and ER motifs showed an improved voltage-dependent fluorescence response. Interestingly, the speed and voltage range of the optical response were also altered with the addition of the export signals. These unintended side effects suggested a potential interruption to the mechanism coupling voltage transients at the plasma membrane to the changes in fluorescence. One potential explanation is that the trafficking motif is restricting the voltage-induced conformational change of the GEVI. Introduction of spacer amino acids between the ER trafficking motif and the FP domain of the GEVI resolved the side effects resulting in a Bongwoori-R3 variant with a 20% increase in fluorescence response to membrane depolarizations while maintaining similar kinetics and voltage range.

MATERIALS AND METHODS

Plasmid DNA construction

Golgi TS and ER ESs from Platisa et al. (6) were adopted for this study. Accordingly, the Golgi TS sequence was located before the beginning of S1 region (from the 71st to 90th amino acid, KSRITSEGEYIPLDQIDINV). A 457-base-pair-long gene fragment containing a Nhe1 site, Golgi TS, and a Cla1 site was commercially synthesized (Integrated DNA Technologies, Coralville, IA). The synthesized fragment was then digested and ligated into Bongwoori-Pos6 and -R3 by using the Nhe1 and Cla1 sites. The ER ES (FCYENEV) was located at the end of Bongwoori-R3 and -Pos6 just before the stop codon. BK27 primer that was designed to have an ER export sequence and a Xho1 site was used to add the ER sequence, thereby Bongwoori-Pos6_ER and Bongwoori-R3_ER were created. Then the two Golgi-TS-sequence-carrying constructs were digested with Nhe1 and Cla1 and ligated into the ER-ES-only variants, resulting in Bongwoori-Pos6_Golgi & ER and Bongwoori-R3_Golgi & ER.

Bongwoori-R3_Golgi & ER_N-term tandem, Bongwoori-R3_Golgi & ER_S2-S3, Bongwoori-R3_Golgi & ER_Linker 1, Bongwoori-R3_Golgi & ER_Linker 2, Bongwoori-R3_Golgi & ER_LP spacer, and Bongwoori-R3_Golgi & ER_6aa spacer (amino acid [aa]) were cloned based on Bongwoori-R3_Golgi & ER by using primers listed in Table S1. The Bongwoori-R3_Golgi & ER_C-term tandem construct was generated by using a commercially synthesized 821-base-pair-long gene fragment. Both the Bongwoori-R3_Golgi & ER_12aa and Bongwoori-R3_Golgi & ER_18aa spacers were prepared by conducting polymerase chain reaction on their 6-amino-acid-long spacer version as a template.

Primers were synthesized by Cosmogenetech (Seoul, South Korea), and generated DNA constructs were analyzed by Bionics (Seoul, South Korea) to verify their gene sequences.

Cell culture and transfection

HEK 293 cells were cultured and transfected following the methods previously described in Lee et al. (25). Briefly, Dulbecco's Modified Eagle Medium (Gibco, New York, NY) with 10% v/v fetal bovine serum (Gibco) was used to incubate HEK 293 cells at 37°C (5% CO_2). For transient transfection of a gene of interest with Lipofectamine 2000 (Invitrogen, Waltham, MA), 0.25% trypsin-EDTA solution (Gibco) was used to suspend the cells, and the cells were plated onto poly-L-lysine-coated (Sigma-Aldrich, Burlington, MA) coverslips (0.08–0.13 mm thick and 10 mm diameter; Ted Pella, Redding, CA) before adding lipofection mixture.

Electrophysiology and voltage imaging

Simultaneous electrophysiology and voltage-imaging experiments of HEK 293 cells were conducted following the protocols described in Lee et al. (25). Briefly, a patch chamber (Warner Instruments, Hamden, CT) sealed with a #0 thickness cover glass was kept at 34°C and perfused with bath solution with the following composition: 150 mM NaCl, 4 mM KCl, 1 mM $MgCl_2$, 2 mM $CaCl_2$, 5 mM D-glucose, and 5 mM HEPES (pH = 7.4). Filamented glass capillaries (1.5 mm [outside diameter]/0.84 mm [inside diameter]; World Precision Instruments, Sarasota, FL) were pulled with resistances of 3–5 MΩ. The pipettes were filled with intracellular solution with the following composition: 120 mM K-aspartate, 4 mM NaCl, 4 mM $MgCl_2$, 1 mM $CaCl_2$, 10 mM EGTA, 3 mM Na_2ATP, and 5 mM HEPES (pH = 7.2). Electrophysiology experiments were conducted using a patch-clamp amplifier (EPC10; HEKA, Reutlingen, Germany). An inverted microscope (IX71; Olympus, Tokyo, Japan) was used for epifluorescence imaging. Collimated light from a Xenon arc lamp (Cairn, Edinburgh, Scotland, UK) was filtered by an excitation filter (FF02-472/30), a dichroic mirror (FF495-Di03), and an emission filter (FF01-497/LP) (all by Semrock, Rochester, NY). A 60× oil-immersion objective lens (1.35 numerical aperture; Olympus) was used for both focusing the excitation light and collecting emitted fluorescence from the cells. Fluorescence signals were recorded at a 1 kHz frame rate by a high-speed CCD camera (NeuroCCD-SMQ; RedShirtImaging, Decatur, GA).

Data acquisition and analyses

Parameters representing voltage-sensing properties of the voltage indicator variants in this paper were first acquired from the raw imaging data by using Neuroplex (RedShirtImaging) and Microsoft Excel (Microsoft, Remond, WA), as previously described in Piao et al. (26) and Lee et al. (25). For each cell, a region of interest corresponding to the plasma membrane was selected, and the pixel intensities were spatially averaged for further analyses. The cellular voltage-imaging results responding to voltage pulses were averaged from 16 trials, as described in Lee et al. (25), except for Bongwoori-Pos6 (12 trials), Bongwoori-R3_ER ES (8 trials), and Bongwoori-Pos6_ER ES (8 trials). The Boltzmann fit analysis to determine the voltage range of each GEVI variant was done by using Origin 9.0 (OriginLab, Northampton, MA) and Microsoft Excel (Microsoft). Time-constants analyses were also conducted in Origin 9.0 (OriginLab). Statistical significance of the means was determined by using Origin 9.0 (OriginLab) and Prism9 (GraphPad, San Diego, CA).

RESULTS

Golgi TS and ER ES motifs improved the dynamic signal size of Bongwoori-R3 and -Pos6 but slowed the response kinetics

The GEVIs Bongwoori-R3 and -Pos6 are ArcLight derivatives that exhibit faster kinetics but a lower dynamic range (25). To improve the dynamic range, Bongwoori variants with different combinations of trafficking motifs were expressed in HEK 293 cells and subjected to whole-cell voltage clamp (Figs. 2 and S1). A considerable slowing of the voltage-dependent optical signal was observed when the ER ES motif was placed at the C-terminus of Bongwoori-R3 (Fig. 2 *A*). Bongwoori-R3 originally had a fast onset time constant of 7 ± 1 ms that accounts for nearly 90% of the optical response (89% ± 3%; Table S2), but Bongwoori-R3_ER ES showed a fast on-tau of 20 ± 3 ms. The percentage of the fast response has also been reduced to 70% ± 4% of the total response, resulting in a significantly slower probe (Fig. S1 *D*). The off-tau for Bongwoori-R3_ER ES was slower as well, yet the dynamic range of Bongwoori-R3_ER ES was increased to 24.8% ± 2.1% ΔF/F/100 mV compared with 20.0% ± 1.3% for Bongwoori-R3.

Similar slowing was also observed for Bongwoori-Pos6 when the ER ES motif was placed at the C-terminus (Fig. S1 *A*). The kinetics of Bongwoori-Pos6 was best fit by a mono-exponential decay function exhibiting an on-tau of 6 ± 1 ms (Table S2). A Bongwoori-Pos6 variant containing only the Golgi TS showed an on-tau of 7 ± 2 ms, similar to the original. However, Bongwoori-Pos6

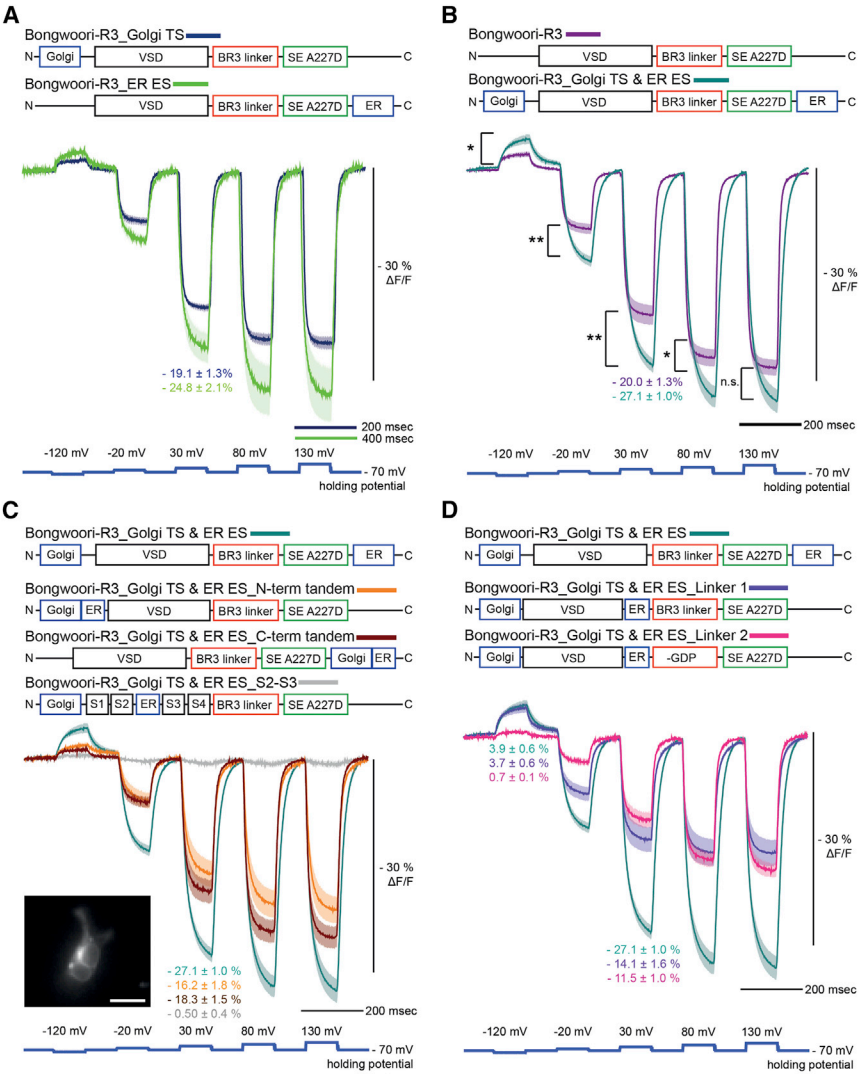

FIGURE 2 Bongwoori-R3 with Golgi TS and/or ER ES at N and C termini. (*A*) Optical response of HEK293 cells expressing variants of Bongwoori-R3 with Golgi TS (N-terminus) or ER ES (C-terminus). Note that the pulse duration for ER ES variant was 200 ms instead of 100 ms. (*B*) Combination of Golgi TS and ER ES for Bongwoori-R3. Bongwoori-R3_Golgi TS & ER ES improved ΔF/F at all tested voltage pulses except for the non-physiological voltage at +130 mV. (*C*) Bongwoori-R3_Golgi TS & ER ES variants with the ER ES relocated to the downstream of the Golgi TS, Golgi TS relocated to the upstream of ER ES at the C-terminus, or ER ES inserted at the S2-S3 loop (intracellular) region. The inset shows a largely intracellular expression pattern of the Bongwoori-R3_Golgi TS & ER ES_S2-S3 construct (scale: 20 μm). (*D*) Bongwoori-R3_Golgi TS & ER ES with the ER ES motif moved in between the VSD and the interdomain linker region or in the linker region but substituting pre-existing linker sequences "YSRQQ" into "FCYENEV." The asterisks represent p values with following criteria; *$p < 0.05$, **$p < 0.01$, and n.s., not significant. The number of cells analyzed are as follows: Bongwoori-R3_Golgi TS: 4; Bongwoori-R3_ER ES: 3; Bongwoori-R3: 5; Bongwoori-R3_Golgi TS & ER ES: 5; Bongwoori-R3_Golgi TS & ER ES_N-term tandem: 5; Bongwoori-R3_Golgi TS & ER ES_C-term tandem: 7; Bongwoori-R3_Golgi TS & ER ES_S2-S3: 3; Bongwoori-R3_Golgi TS & ER ES: 5; Bongwoori-R3_Golgi TS & ER ES_Linker 1: 5; and Bongwoori-R3_Golgi TS & ER ES_Linker 2: 5.

with ER ES near the C-terminus introduced a slow component to the voltage-dependent optical signal, yielding an optical signal best fit by a bi-exponential function with a weighted on-tau of 23 ± 1 ms (Table S2; Fig. S1 *A* and *D*). The fast component was also slower (12 ± 1 ms) and only constituted 61% ± 6% of the overall response. The off-tau was also slowed from 7 ± 1 ms for Bongwoori-Pos6 to 28 ± 1 ms for Bongwoori-Pos6_ER ES, while both responses were best fit by a mono-exponential decay function.

Introducing both Golgi TS and ER ES motifs for Bongwoori-R3 and -Pos6 showed similar results compared with versions containing only the ER ES motif (Figs. 2 *B* and S1 *B*). Bongwoori-R3_Golgi TS & ER ES showed significantly larger ΔF/F values at physiological voltage ranges (Figs. 2 *B* and S1 *C*). However, similar to the ER-ES-only version, the response speeds were notably slower (Fig. 2 *B*). Since Bongwoori-Pos6, with the two membrane-trafficking signals, did not show notable improvements other than one hyperpolarizing voltage pulse (Fig. S1 *B*), we focused on Bongwoori-R3 variants.

Altering the location of the ER ES resulted in a diminished ΔF/F for Bongwoori-R3 variants

Both Bongwoori-Pos6 and -R3 variants containing the ER motif showed slower responses to voltage transients (Fig. S1 *D*; Table S2). Since the ER ES motif was located at the C-terminus of the FP domain, we hypothesized that the trafficking machinery may still be bound to the ER ES motif at the plasma membrane, creating a drag on the movement of S4 in response to voltage transients at the plasma membrane. To test if this can be ameliorated while keeping the increased ΔF/F, the ER motif was moved to different locations within the Bongwoori-R3_Golgi TS & ER ES construct. First, the ER motif was relocated upstream of S1 at the 91st amino acid

region, substituting the 7 amino acids from "DDGRMEI" into "FCYENEV." We named this variant Bongwoori-R3_Golgi TS & ER ES_N-term tandem (Fig. 2 *C*). The next variant was designed to have both motifs in tandem at the C-terminus as reported for some opsin-FRET-type voltage sensors (7,27). The cytoplasmic S2-S3 loop region was also tested as an ER ES insertion location. All three variants exhibited diminished fluorescence responses compared with Bongwoori-R3_Golgi TS & ER ES. The variant with the ER motif at the S2-S3 loop was almost completely insensitive to membrane-potential changes (Fig. 2 *C*, *gray trace*). The expression pattern of this construct in HEK 293 cells appeared largely intracellular and not localized to the membrane, suggesting a possible protein-folding issue (Fig. 2 *C*, *inset*).

The cytoplasmic linker between the VSD and the FP was also considered for an ER ES insertion site (Fig. 2 *D*). Two linker variants were generated either by simply adding the seven amino acid ER motif at the linker region (Bongwoori-R3_Golgi TS & ER ES_Linker 1) or by substituting some of the amino acid residues of the linker from "YSRQQ" into "FCYENEV" (Bongwoori-R3_Golgi TS & ER ES_Linker 2) to keep it close to the original linker length of Bongwoori-R3. Linker variant 1 maintained Bongwoori-R3_Golgi TS & ER ES's fluorescence signal size during membrane hyperpolarization but not during membrane depolarizations, resulting in a negatively shifted $V_{1/2}$ value of -38 ± 1 mV (Figs. 2 *D* and S2 *A*; Table S2). The second linker variant that has two additional linker amino acids showed decreased fluorescence responses across the entire voltage range tested. This seems to have been at least partially caused by its right-shifted voltage range (16 ± 1 mV; Table S2). However, given that the maximal signal is also greatly reduced, the altered linker length may also have changed the electrostatic interactions between neighboring FP domains that have been shown to affect the activity of ArcLight-derived GEVIs (28). Except for the version that had the ER motif at S2-S3 loop, where it was difficult to fit the fluorescence trace to any exponential decay function, the other four variants all showed more improved time constants than Bongwoori-R3_Golgi TS & ER ES, at least in either on or off responses (Fig. S2 *B*). However, none of these maintained the dynamic range of Bongowori-R3_Golgi TS & ER ES during membrane depolarizations.

Inserting non-helical, flexible amino acid spacers between the FP and the C-terminal ER ES motif recovered the kinetics and responsive voltage range

An alternate way to resolve the slow kinetics issue would be to introduce a short spacer sequence to relieve potential restrictions imposed by the trafficking motif on voltage-induced conformational changes. Akerboom et al. (29) previously reported that they used leucine and proline between the circularly permuted green fluorescent protein and calmodulin to improve the dynamic range of GCaMP3, which proved successful for GcaMP5s, GcaMP6s, and GcaMP6f (29,30). Bongwoori-R3_Golgi TS & ER ES with the leucine/proline insertion showed comparable voltage-dependent fluorescence responses (Fig. 3 *A* and *C*). However, the on and off time constants at the 100 mV depolarization step were still slow (Fig. 3 *D*).

A six-amino-acid-long sequence (GGTGGS) devoid of a secondary structure has been employed for both genetically encoded calcium indicator and GEVI optical probes (31–33) as well as connecting the N and C termini of the circularly permuted green fluorescent protein (34). The Bongwoori-R3_Golgi TS & ER ES_6aa spacer showed a decreased dynamic response to membrane depolarization than the version having the trafficking motifs but lacking the spacer (Fig. 3 *A*). Interestingly, however, the GGTGGS spacer improved the response speed. The time constant for onset at 100 mV depolarization was 15 ± 1 ms (fast component: 9 ± 2 ms [$81\% \pm 3\%$]), which was faster than Bongwoori-R3_Golgi TS & ER ES (Fig. 3 *A* and *D*; Table S2).

Although the flexible 6-amino-acid-long spacer showed some improvements, the ΔF/F/100 mV was still about 5% smaller than Bongwoori-R3_Golgi TS & ER ES, and the off-kinetics (weighted tau off: 16 ± 1 ms) were still slower than Bongwoori-R3 (10 ± 2 ms) (Table S2). We therefore tried 12 amino acid (GGTGGSGGTGGS) and 18 amino acid (GGTGGSGGTGGSGGTGGS) spacers to see if extended spacer lengths would further improve the kinetics (Fig. 3 *B*). Both versions showed increased ΔF/F/100 mV depolarization that was comparable to the signal size of Bongwoori-R3_Golgi TS & ER ES (Fig. 3 *C*). In terms of kinetics, the two variants were faster for both on and off time constants, unlike the 6-amino-acid version (Fig. 3 *B* and *D*; Table S2). This demonstrated that a flexible spacer of sufficient length alleviated the side effects of having an ER ES at the C-terminus of the fluorescent reporter.

Fitting the fluorescence traces of the variants with membrane-trafficking motifs to the Boltzmann function revealed that Golgi TS & ER ES sequences shifted responsive voltage ranges. This resulted in negatively shifted $V_{1/2}$ values for both Bongwoori-Pos6 and -R3 variants (-43 ± 4 and -20 ± 1 mV, respectively) (Fig. 4 *A* and *B*). In terms of imaging the suprathreshold activity of a neuron, this change may be disadvantageous for Bongwoori-Pos6 since its original voltage range was already tuned toward subthreshold activity ($V_{1/2}$ at -28 ± 3 mV). The $V_{1/2}$ of Bongwoori-R3_Golgi TS & ER ES was also shifted about 17 mV to more negative potentials. It is therefore noteworthy that this

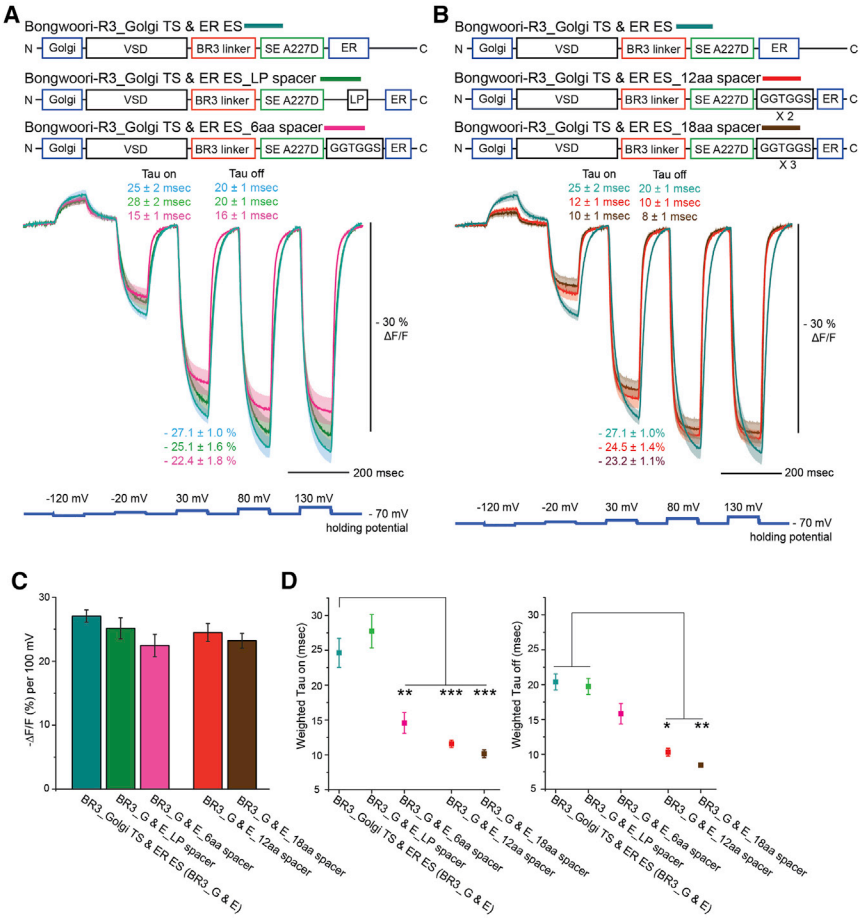

FIGURE 3 Insertion of inter-domain spacers recovered the kinetics while maintaining the improved ΔF/F amplitudes. (*A*) Bongwoori_R3_Golgi TS & ER ES variants with two- and six-amino-acid-long inter-domain spacers. (*B*) Bongwoori-R3_Golgi TS & ER ES variants with extended flexible inter-domain linkers comprised of "GGTGGS" from the circularly permuted green fluorescent protein design. (*C*) Comparison of ΔF/F amplitudes per 100 mV (−70 to +30 mV). (*D*) Comparison of on- and off-response kinetics upon 100 mV voltage pulse. Note that the on-response kinetics was improved for all three variants having "GGTGGS" spacer sequences. The statistics in (*D*, *right*) were done with Kruskal-Wallis ANOVA followed by Dunn's multiple comparison test. The asterisks in (*D*) are p values with the following criteria: *$p < 0.05$, **$p < 0.01$, and ***$p < 0.001$. Shades are mean ± SE. The number of cells analyzed are as follows: Bongwoori-R3_Golgi TS & ER ES: 5; Bongwoori-R3_Golgi TS & ER ES_LP spacer: 7; Bongwoori-R3_Golgi TS & ER ES_6aa spacer: 8; Bongwoori-R3_Golgi TS & ER ES_12aa spacer: 6; and Bongwoori-R3_Golgi TS & ER ES_18aa spacer: 5. The time constants shown above the fluorescence traces are weighted tau values.

Bongwoori-R3 variant still exhibited increased ΔF/F at depolarized membrane potentials despite the response range biasing toward more negative membrane potentials, indicating a potential for a larger dynamic range of the GEVI.

Increasing the distance and the flexibility between the FP and the ER ES by inserting a flexible spacer sequence mitigated the voltage-range shift as well as the slow response kinetics (Fig. 4 *B* and *C*). When the spacer length was increased to 18 amino acids, the voltage range returned close to the $V_{1/2}$ value of Bongwoori-R3, whereas the 6-amino-acid-spacer variant's $V_{1/2}$ value was similar to that of Bongwoori-R3_Golgi TS & ER ES (Fig. 4 *B*).

DISCUSSION

In this study, we explored the effects of introducing Kir2.1-derived membrane-trafficking sequences into Bongwoori family GEVIs and observed a larger fluorescence dynamic range upon a membrane-potential change. However, the addition of these trafficking motifs resulted in unexpected effects on the kinetics and responsive voltage ranges. In terms of insertion sites, introducing a Golgi TS upstream of the transmembrane region of the VSD and an ER ES at the C-terminus of Bongwoori-R3 gave the largest increase in ΔF/F. For Bongwoori-R3, having just the Golgi TS alone did not make a noticeable change to the voltage-dependent optical signal, but having the ER ES did. Interestingly, although the Golgi TS did not seem to have a notable effect by itself, when it was introduced together with the ER ES to Bongwoori-R3 (Bongwoori-R3_Golgi TS & ER ES), it did improve the onset kinetics per 100 mV depolarization compared with the ER-ES-only version (Bongwoori-R3_ER ES; Figs. 2 *B* and S1 *D*). The difference between Bongwoori-Pos6_Golgi TS & ER ES and Bongwoori-R3_Golgi TS & ER ES was also interesting since the two are only different in the linker composition fusing the FP to the VSD (Bongwoori-Pos6's linker is 1 aa longer and has 3 more arginines than that of Bongwoori-R3).

The position of the trafficking motifs in Bongwoori-R3 mattered. Bongwoori-R3_Golgi TS & ER ES showed improved voltage-dependent fluorescence changes when the ER ES was inserted at the C-terminus of super

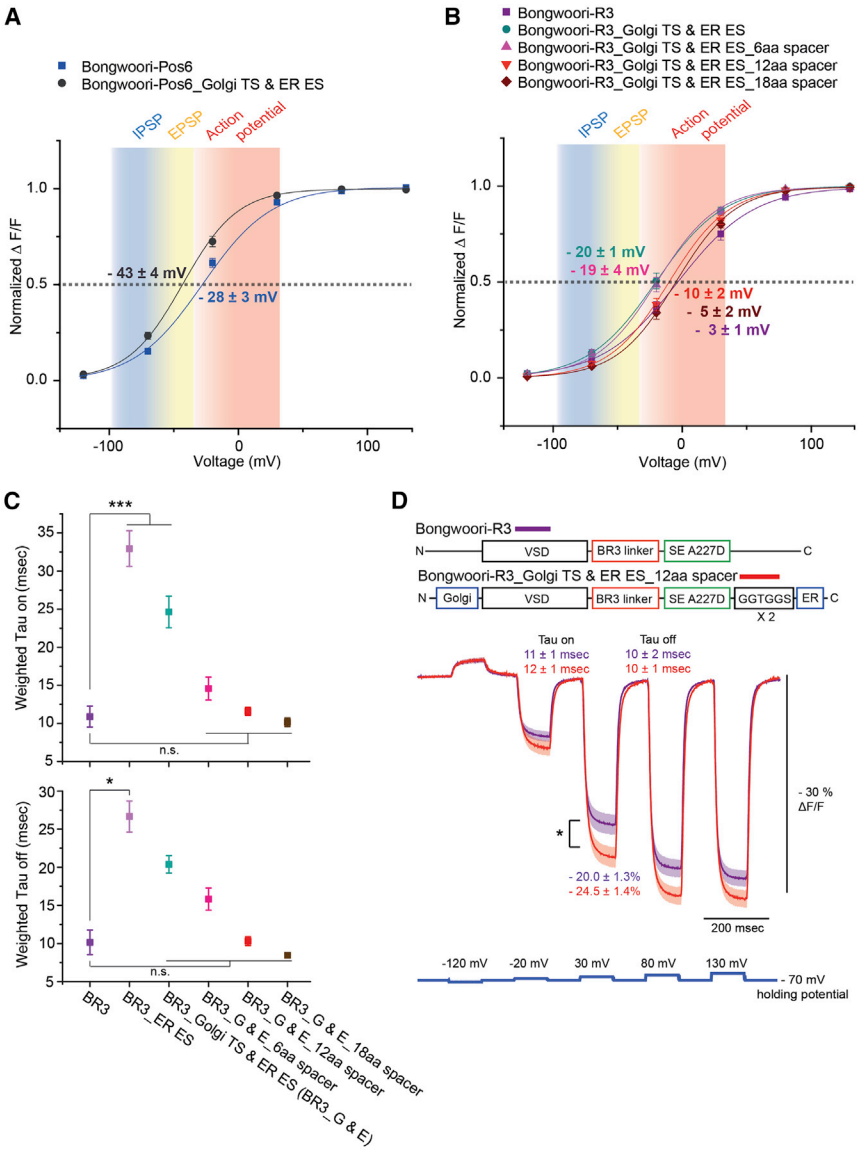

FIGURE 4 Consequences of Golgi TS and ER ES additions to Bongwoori-Pos6 and -R3 and alleviation of resulted effects by introducing inter-domain spacers for voltage dependency and kinetic responses. (*A* and *B*) Normalized fluorescence to voltage curves for Bongwoori-Pos6 and -R3 variants. Note that for both Bongwoori-Pos6 and -R3, the addition of Golgi TS and ER ES left-shifted the voltage-dependence curves. For Bongwoori-R3_Golgi TS & ER ES variants with the inter-domain spacers, the left-shifted $V_{1/2}$ values were recovered back toward the original value (−3 ± 1 mV). (*C*) The same variants shown in (*B*) but for weighted on-response kinetics (*top panel*) and off-response kinetics (*bottom panel*). The slow kinetics of Bongwoori-R3_Golgi TS & ER ES are apparent but then mitigated by the addition of the spacers. (*D*) A direct comparison of the Bongwoori-R3_Golgi TS & ER ES_12aa spacer with Bongwoori-R3. The statistics in (*C*, *bottom*) were done with Kruskal-Wallis ANOVA followed by Dunn's multiple comparison test. Shades are mean ± SE. The asterisks in (*C*) and (*D*) are p values with the following criteria: *$p < 0.05$, **$p < 0.01$, and ***$p < 0.001$. The number of cells analyzed are as follows: Bongwoori-R3: 5; Bongwoori-R3_Golgi TS & ER ES_12aa spacer: 6; Bongwoori-R3_Golgi TS & ER ES: 5; Bongwoori-R3_Golgi TS & ER ES_6aa spacer: 8; and Bongwoori-R3_Golgi TS & ER ES_18aa spacer: 5.

ecliptic pHluorin A227D. Relocating the motifs to different regions showed some improvements in kinetics but at the expense of the improved ΔF/F (Fig. S2). Instead, introducing a flexible spacer encoding GGTGGS alleviated the slower response. Increasing the length of that spacer between the FP and the ER ES sequence further improved the kinetics to that of the original Bongwoori-R3 while preserving the increase in ΔF/F for a 100 mV depolarization. In terms of the voltage range, Bongwoori-Pos6 and -R3, with the two membrane-targeting motifs, showed 15 and 17 mV negatively shifted $V_{1/2}$ values, respectively. Extending the flexible spacer from 6 amino acids to 12 and 18 shifted the voltage range back to near the original $V_{1/2}$ (Fig. 4 *B*; Table S2). It was interesting that insertion of the flexible spacer both improved the kinetics and recovered the $V_{1/2}$ close to the original Bongwoori-R3 while maintaining the increase in the dynamic range (Fig. 4 *B*–*D*). This suggests that changes in the two voltage-sensing properties might have been caused by the same restraint mechanism caused by the ER ES to these GEVIs.

The two Kir2.1-derived sequences were expected to improve membrane trafficking and in turn, reduce the level of voltage-insensitive intracellular expression of Bongwoori family GEVIs. While the addition of these motifs did improve the voltage-dependent optical signal, we also observed undesired effects on the speed and voltage range of the GEVI, especially with the addition of the ER ES sequence at the C-terminus. A recent publication also introduced these trafficking motifs at similar positions to another version of

ArcLight, resulting in the novel GEVI ArcLight-ST (24). The presence of the ER ES motif in ArcLight-ST also slowed the voltage-dependent optical signal, making it impossible to differentiate action potentials from subthreshold activity. A clever approach by co-expressing ArcLight-ST with a red-shifted calcium indicator enables the resolution of suprathreshold activity from subthreshold voltage changes. It is unclear if the ER ES motif shifted the voltage dependence of ArcLight-ST since the introduction of the trafficking motif was done in combination with a mutation to the VSD. However, the introduction of a spacer region between the C-terminal trafficking signal and the FP domain should return the speed and may negate the need for a calcium sensor to resolve action potentials. The fluorescence response of Bongwoori-Pos6_ER ES alone showed this voltage shift since the larger fluorescence modulation was only seen during a hyperpolarizing voltage pulse but not during depolarizing ones (Fig. S1 *A* and *B*). If the improved dynamic range was solely a result of better membrane trafficking, larger $\Delta F/F$ values should have been observed at all voltage pulses tested. The effects on kinetics and voltage range being rectified by the insertion of flexible linkers into Bongwoori-R3-Golgi TS & ER ES lead to a hypothesis that the seven-amino-acid-long sequence of the ER ES containing the di-acidic motif (-ENE-) plays an anchor-like role in the voltage-sensing and fluorescence change of Bongwoori-like GEVIs (10,11,35). This can be attributed to a membrane-bound component persisting once the protein has been delivered to the plasma membrane.

The mechanism that mediates a fluorescence change upon depolarization of the plasma membrane for the Bongwoori family of GEVIs is not completely understood. Movement of S4 in the VSD has been shown to correlate with the fluorescence change (36–38). Here, we show that introducing a trafficking motif at the C-terminus slows the response and alters the voltage range of the GEVI. ArcLight-ST exhibits similar characteristics (24). There are several potential explanations for the change in the voltage-dependent signal. It is possible that the ER ES at the C-terminus is interacting with other domains of the GEVI (or nearby proteins) that affect the voltage-induced conformational change. It is also possible that the ER ES motif is interacting with the plasma membrane in some manner that would also affect the functioning of the GEVI. Another potential explanation is that the trafficking machinery remains associated with the motif, resulting in a hindrance to the movement of the FP domain of the GEVI. All three possibilities could potentially be addressed by introducing a flexible stretch of amino acids between the FP domain and the trafficking motif. While we were successful in rescuing the speed and the voltage range of the sensor while maintaining the improved dynamic range, biochemical studies and structural determinations will be required to better appreciate how the ER ES motif alters the functioning of the GEVI. The ability to optically monitor voltage-induced conformational changes to the Bongwoori family of GEVIs has allowed us to visualize a potential, persistent protein interaction at the plasma membrane and could provide further insights into how the cell functions as well as into the development of better GEVIs.

SUPPORTING MATERIAL

Supporting material can be found online at https://doi.org/10.1016/j.bpr.2022.100047.

AUTHOR CONTRIBUTIONS

B.E.K. designed and performed experiments. S.L. designed and performed experiments, analyzed data, and wrote the manuscript. Y.-K.S. analyzed data and assisted with the writing. B.J.B. designed experiments, analyzed data, and assisted with the writing of the manuscript. All authors reviewed the manuscript.

DECLARATION OF INTERESTS

The authors declare no competing interests.

ACKNOWLEDGMENTS

We thank Dr. Lawrence Cohen for a critical review of the manuscript. This study was funded by Korea Institute of Science and Technology grant 2E30963. S.L. was supported by the Global PhD Fellowship program (NRF-2013H1A2A1033344) of the National Research Foundation (NRF), Ministry of Education (Korea). B.K. was supported by the Basic Science Research Program through the National Research Foundation (NRF-2N63220) of the Ministry of Education (Korea). The research was also supported by Basic Science Research Program (NRF-2015R1D1A1A01060569) through the National Research Foundation of Korea, Ministry of Education.

REFERENCES

1. Peterka, D. S., H. Takahashi, and R. Yuste. 2011. Imaging voltage in neurons. *Neuron.* 69:9–21. https://doi.org/10.1016/j.neuron.2010.12.010.
2. Nakajima, R., A. Jung, …, B. J. Baker. 2016. Optogenetic monitoring of synaptic activity with genetically encoded voltage indicators. *Front. Synaptic Neurosci.* 8:1–9. https://doi.org/10.3389/fnsyn.2016.00022.
3. Gradinaru, V., K. R. Thompson, and K. Deisseroth. 2008. eNpHR: a natronomonas halorhodopsin enhanced for optogenetic applications. *Brain Cell Biol.* 36:129–139. https://doi.org/10.1007/s11068-008-9027-6.
4. Gradinaru, V., F. Zhang, …, K. Deisseroth. 2010. Molecular and cellular approaches for diversifying and extending optogenetics. *Cell.* 141:154–165. https://doi.org/10.1016/j.cell.2010.02.037.

5. Akemann, W., H. Mutoh, …, T. Knöpfel. 2012. Imaging neural circuit dynamics with a voltage-sensitive fluorescent protein. *J. Neurophysiol.* 108:2323–2337. https://doi.org/10.1152/jn.00452.2012.

6. Platisa, J., G. Vasan, …, V. A. Pieribone. 2017. Directed evolution of key residues in fluorescent protein inverses the polarity of voltage sensitivity in the genetically encoded indicator ArcLight. *ACS Chem. Neurosci.* 8:513–523. https://doi.org/10.1021/acschemneuro.6b00234.

7. Gong, Y., C. Huang, …, M. J. Schnitzer. 2015. High-speed recording of neural spikes in awake mice and flies with a fluorescent voltage sensor. *Science.* 350:1361–1366. https://doi.org/10.1126/science.aab0810.

8. Adam, Y., J. J. Kim, …, A. E. Cohen. 2019. Voltage imaging and optogenetics reveal behaviour-dependent changes in hippocampal dynamics. *Nature.* 569:413–417. https://doi.org/10.1038/s41586-019-1166-7.

9. Pegan, S., C. Arrabit, …, S. Choe. 2005. Cytoplasmic domain structures of Kir2.1 and Kir3.1 show sites for modulating gating and rectification. *Nat. Neurosci.* 8:279–287. https://doi.org/10.1038/nn1411.

10. Stockklausner, C., J. Ludwig, …, N. Klöcker. 2001. A sequence motif responsible for ER export and surface expression of Kir2.0 inward rectifier K+ channels. *FEBS Lett.* 493:129–133. https://doi.org/10.1016/S0014-5793(01)02286-4.

11. Ma, D., N. Zerangue, …, L. Y. Jan. 2001. Role of ER export signals in controlling surface potassium channel numbers. *Science.* 291:316–319. https://doi.org/10.1126/science.291.5502.316.

12. Ma, D., and L. Y. Jan. 2002. ER transport signals and trafficking of potassium channels and receptors. *Curr. Opin. Neurobiol.* 12:287–292. https://doi.org/10.1016/S0959-4388(02)00319-7.

13. Stockklausner, C., and N. Klöcker. 2003. Surface expression of inward rectifier potassium channels is controlled by selective Golgi export. *J. Biol. Chem.* 278:17000–17005. https://doi.org/10.1074/jbc.M212243200.

14. Hofherr, A., B. Fakler, and N. Klöcker. 2005. Selective Golgi export of Kir2.1 controls the stoichiometry of functional Kir2.x channel heteromers. *J. Cell Sci.* 118:1935–1943. https://doi.org/10.1242/jcs.02322.

15. Ma, D., T. K. Taneja, …, P. A. Welling. 2011. Golgi export of the Kir2.1 channel is driven by a trafficking signal located within its tertiary structure. *Cell.* 145:1102–1115. https://doi.org/10.1016/j.cell.2011.06.007.

16. Li, X., B. Ortega, …, P. A. Welling. 2016. A common signal patch drives ap-1 protein-dependent golgi export of inwardly rectifying potassium channels. *J. Biol. Chem.* 291:14963–14972. https://doi.org/10.1074/jbc.M116.729822.

17. Ma, D., N. Zerangue, …, L. Y. Jan. 2002. Diverse trafficking patterns due to multiple traffic motifs in G protein-activated inwardly rectifying potassium channels from brain and heart. *Neuron.* 33:715–729. https://doi.org/10.1016/S0896-6273(02)00614-1.

18. Zhang, F., L.-P. Wang, …, K. Deisseroth. 2007. Multimodal fast optical interrogation of neural circuitry. *Nature.* 446:633–639. https://doi.org/10.1038/nature05744.

19. Kwon, T., M. Sakamoto, …, R. Yuste. 2017. Attenuation of synaptic potentials in dendritic spines. *Cell Rep.* 20:1100–1110. https://doi.org/10.1016/j.celrep.2017.07.012.

20. Bando, Y., M. Sakamoto, …, R. Yuste. 2019. Comparative evaluation of genetically encoded voltage indicators. *Cell Rep.* 26:802–813.e4. https://doi.org/10.1016/j.celrep.2018.12.088.

21. Piatkevich, K. D., S. Bensussen, …, X. Han. 2019. Population imaging of neural activity in awake behaving mice. *Nature.* 574:413–417. https://doi.org/10.1038/s41586-019-1641-1.

22. Abdelfattah, A. S., T. Kawashima, …, E. R. Schreiter. 2019. Bright and photostable chemigenetic indicators for extended in vivo voltage imaging. *Science.* 365:699–704. https://doi.org/10.1126/science.aav6416.

23. Villette, V., M. Chavarha, …, M. Z. Lin. 2019. Ultrafast two-photon imaging of a high-gain voltage indicator in awake behaving mice. *Cell.* 179:1590–1608.e23. https://doi.org/10.1016/j.cell.2019.11.004.

24. Bando, Y., M. Wenzel, and R. Yuste. 2021. Simultaneous two-photon imaging of action potentials and subthreshold inputs in vivo. *Nat. Commun.* 12:7229. https://doi.org/10.1038/s41467-021-27444-9.

25. Lee, S., T. Geiller, …, B. J. Baker. 2017. Improving a genetically encoded voltage indicator by modifying the cytoplasmic charge composition. *Sci. Rep.* 7:8286. https://doi.org/10.1038/s41598-017-08731-2.

26. Piao, H. H., D. Rajakumar, …, B. J. Baker. 2015. Combinatorial mutagenesis of the voltage-sensing domain enables the optical resolution of action potentials firing at 60 Hz by a genetically encoded fluorescent sensor of membrane potential. *J. Neurosci.* 35:372–385. https://doi.org/10.1523/JNEUROSCI.3008-14.2015.

27. Gong, Y., M. J. Wagner, …, M. J. Schnitzer. 2014. Imaging neural spiking in brain tissue using FRET-opsin protein voltage sensors. *Nat. Commun.* 5:3674. https://doi.org/10.1038/ncomms4674.

28. Kang, B. E., L. M. Leong, …, B. J. Baker. 2021. Mechanism of ArcLight derived GEVIs involves electrostatic interactions that can affect proton wires. *Biophys. J.* 1–11. https://doi.org/10.1016/j.bpj.2021.03.009.

29. Akerboom, J., T. Chen, …, L. L. Looger. 2012. Optimization of a GCaMP calcium indicator for neural activity imaging. *J. Neurosci.* 32:13819–13840.

30. Chen, T.-W., T. J. Wardill, …, D. S. Kim. 2013. Ultrasensitive fluorescent proteins for imaging neuronal activity. *Nature.* 499:295–300. https://doi.org/10.1038/nature12354.

31. Nakai, J., M. Ohkura, and K. Imoto. 2001. A high signal-to-noise Ca(2+) probe composed of a single green fluorescent protein. *Nat. Biotechnol.* 19:137–141. https://doi.org/10.1038/84397.

32. Tian, L., S. A. Hires, …, L. L. Looger. 2009. Imaging neural activity in worms, flies and mice with improved GCaMP calcium indicators. *Nat. Methods.* 6:875–881. https://doi.org/10.1038/nmeth.1398.

33. St-Pierre, F., J. D. Marshall, …, M. Z. Lin. 2014. High-fidelity optical reporting of neuronal electrical activity with an ultrafast fluorescent voltage sensor. *Nat. Neurosci.* 17:884–889. https://doi.org/10.1038/nn.3709.

34. Baird, G. S., D. A. Zacharias, and R. Y. Tsien. 1999. Circular permutation and receptor insertion within green fluorescent proteins. *Proc. Natl. Acad. Sci. U S A.* 96:11241–11246. https://doi.org/10.1073/pnas.96.20.11241.

35. Capera, J., C. Serrano-Novillo, …, A. Felipe. 2019. The potassium channel odyssey: mechanisms of traffic and membrane arrangement. *Int. J. Mol. Sci.* 20. https://doi.org/10.3390/ijms20030734.

36. Treger, J. S., M. F. Priest, and F. Bezanilla. 2015. Single-molecule fluorimetry and gating currents inspire an improved optical voltage indicator. *Elife.* 4:1–18. https://doi.org/10.7554/eLife.10482.

37. Villalba-Galea, C. A., W. Sandtner, …, F. Bezanilla. 2008. S4-based voltage sensors have three major conformations. *Proc. Natl. Acad. Sci. U S A.* 105:17600–17607. https://doi.org/10.1073/pnas.0807387105.

38. Lundby, A., W. Akemann, and T. Knöpfel. 2010. Biophysical characterization of the fluorescent protein voltage probe VSFP2.3 based on the voltage-sensing domain of Ci-VSP. *Eur. Biophys. J.* 39:1625–1635. https://doi.org/10.1007/s00249-010-0620-0.